Contributions of rhodopsin, cone opsins, and melanopsin to postreceptoral pathways inferred from natural image statistics

Pablo A. Barrionuevo and **Dingcai Cao**[*]

Department of Ophthalmology and Visual Sciences, University of Illinois at Chicago, 1905 West Taylor Street, Chicago, Illinois 60612, USA

Abstract

Visual neural representation is constrained by the statistical properties of the environment. Prior analysis of cone pigment excitations for natural images revealed three principal components corresponding to the major retinogeniculate pathways identified by anatomical and physiological studies in primates. Here, principal component analyses were conducted on the excitations of rhodopsin, cone opsins, and melanopsin for nine hyperspectral images under 21 natural illuminants. The results suggested that rhodopsin and melanopsin may contribute to the three major retinogeniculate pathways. Rhodopsin and melanopsin may provide additional constraints in natural scene statistics, leading to new components that cannot be revealed by analysis based on cone opsin excitations only.

1. INTRODUCTION

Anatomical and physiological studies in primates have identified three major retinogeniculate pathways that transfer visual information from the retina to the brain for image-forming processing, i.e., the magnocellular (MC-), parvocellular (PC-), and koniocellular (KC-), pathways [1,2]. These pathways combine differential long (L-), middle (M-), and short (S-) wavelength-sensitive cone excitations [3–5]. The MC-pathway processes summed L- and M-cone excitations to signal luminance information. The PC-pathway processes the difference in L- and M-cone excitations to contribute to the "red-green" chromatic opponency signal. The KC-pathway processes the responses of S-cones opposed to the sum of L- and M-cones to contribute to the "blue-yellow" chromatic information. The evolution of these visual pathways for specific neural coding and representation is thought to be constrained by the statistical properties of the natural visual environment (e.g., [6,7]). Theoretically, opponent spectral processing of cone excitations removes redundant information to produce efficient coding [8,9]. Indeed, a principal component analysis (PCA) of cone pigment excitations on natural images revealed three principal components that are consistent with the combinations of cone inputs in the three major retinogeniculate pathways [8]. However, these prior analyses have rarely considered the contribution from rods, which are operating simultaneously with cones at mesopic lighting conditions and may play an important role in color vision evolution [10,11].

[*]Corresponding author: dcao98@uic.edu.

Trichromacy, which is mainly present in diurnal primates, also indicates rods may contribute to the evolution of the postreceptoral pathways [12].

Since rods evolved after cones, it is likely that the rod circuitry was attached onto the existing cone pathways [13]. In the primate retina, two rod pathways have been identified [14,15], one via rods to rod bipolars and AII amacrine cells to cone bipolar cells and the other via rod-cone gap junctions to cone bipolar cells. The sharing of neural pathways between rods and cones implies that rods must have inputs to all three major retinogeniculate pathways [16]. Physiological studies have shown there is strong rod input to the MC-pathway [17–22] and weak rod input to the PC-pathway [19,23]. Two recent studies have demonstrated strong rod input to the bistratified ganglion cells in the KC-pathway in the peripheral retina [24,25]. Psychophysical studies also demonstrated rods could contribute to all three retinogeniculate pathways, depending on the adaptation level [26–28]. From an information theory perspective, it has been suggested that the number of photopigments and their spectral activation locations are limited by the comb-filtered spectral frequency in the visual spectrum, and three or four photopigments are sufficient to code spectral information in primates [29]. When photoreceptor noise is considered, it is predicted that either trichromacy or dichromacy could code spectral information in the visible spectrum efficiently [30]. It is unknown whether rod input to the retinogeniculate pathways can be revealed by natural image analysis and whether adding rod signals would provide additional constraints for postreceptoral neural coding and representation. The primary aim of this study was to assess how rod and cone inputs are combined to contribute to different postreceptoral pathways from the perspective of natural image statistics.

In addition, a newly identified retinal photopigment, i.e., melanopsin, is expressed in the intrinsically photosensitive retinal ganglion cells (ipRGCs) in rodents and primates [31–33]. Cells that contain melanopsin innervate nonimage-forming neural centers to control the circadian rhythm and pupil responses [34–37]. These melanopsin-containing cells also receive inputs from rods and cones, and it has been suggested that ipRGCs also contribute to image-forming visual processing [38,39]. It is unclear whether melanopsin activation contributes to the three retinogeniculate pathways for image-forming processing. The secondary aim of this study was to assess optimal combinations of the rhodopsin, cone opsins, and melanopsin excitations from natural image statistics. We first replicated cone-opsin-based analysis and then expanded our analyses by including rhodopsin and melanopsin inputs.

2. METHODS

A. Natural Images and Illuminants

The excitation of each type of photopigment was computed from the combination of the reflectance of hyperspectral images with natural illuminants. Nine hyperspectral images of rural scenes were downloaded from the website (http://personalpages.manchester.ac.uk/staff/david.foster/default.htm) of Dr. David Foster's laboratory [40]. These images contained primordial foliage and spectral reflectance information at each pixel. The first four images (sizes of 820×820 pixels) were Scenes 1–4 from "hyperspectral images of natural scenes 2002," which were acquired using a tunable bi-refringent filter mounted in front of the lens

of a progressive-scanning monochrome digital camera [41]. The last five (sizes of 1017 × 1267 pixels) were Scenes 1–5 from "hyperspectral images of natural scenes 2004," which were acquired using a fast-tunable liquid-crystal filter and a low-noise Peltier-cooled digital camera [42].

Natural illuminations were represented by 21 "D" illuminants with a correlated color temperature (CCT) from 3600 to 25,000 K [43], covering different phases of the day from moonlight to sunlight [44,45]. Four representative illuminant spectral distributions are shown in Fig. 1(a). Note that the correspondence between CCT values and the phases of a day is only approximate, since the natural-light CCT depends on factors, such as time of the year, location, and atmospheric conditions [44,46]. Subsequent PCA requires zero-mean input variables; therefore the spectral power distributions of the illuminants were normalized so that the values were between 0 and 1. The normalization of illuminants would not affect the weights of the components, as shown in Eqs. (1) and (2).

B. Analysis

For a combination of illuminant and scene, at each pixel the illuminant power was multiplied by the reflectance value at each wavelength to obtain the spectral radiance values of the pixel. We then computed the excitations of five photopigments (L-cone, M-cone, and S-cone opsins, rhodopsin, and melanopsin) at each pixel. The cone opsin excitations (L, M, S) were computed based on the Smith–Pokorny cone fundamentals for the CIE 1964 10° Standard Observer [47]. Rhodopsin excitation (R) was computed based on the scotopic luminosity function [48]. The melanopsin excitation (I) was computed according to the melanopsin spectral-sensitivity function [49]. The spectral-sensitivity functions of the photopigments were normalized [Fig. 1(b)] such that for an equal-energy-spectrum light at 1 Td, the L-, M-, and S-cone opsins, rhodopsin, and melanopsin excitations would be 0.667 (L), 0.333 (M), 1 (S), 1 (R), and 1 (I) Td, respectively, (so L + M = 1 Td). The photopigment excitations (in the same units) were calculated for the range 400–700 nm in 10 nm steps.

PCA was used to reveal underlying linearly uncorrelated components [50]. PCA requires the data to have a normal distribution and a mean of zero; therefore a logarithmic transformation was performed on the data to reduce skewness:

$$E = log\,(E_O) - \mathrm{mean}\,[log\,(E_O)], \quad (1)$$

where E_O is the computed raw photopigment excitation (L_O, M_O, S_O, R_O, or I_O), and E is the transformed excitation (*L, M, S, R,* or *I*, respectively). Note the normalization in Eq. (1) also ensured that the choice of the unit for each photopigment excitation (E_O) could be arbitrary since a linear scaling of E_O by a factor k results in an identical value of E:

$$log\,(kE_O) - \mathrm{mean}\,[log\,(kE_O)] = log\,(k) + log\,(Eo) - log\,(k) - \mathrm{mean}\,[log\,(Eo)] = E. \quad (2)$$

PCA allows determination of new orthogonal axes (uncorrelated) through linear combination of the transformed excitations:

$$P = \sum_{1}^{n} f_i * E_i, \quad \text{(3)}$$

where P is a specific principal component, f_i is the coefficient for a photopigment excitation E_i, and n is the total number of photopigments included in the analysis and is also the maximum number of principal components. Note that the variance-covariance structure in photopigment excitations, which is largely determined by the width and location of the spectral-sensitivity functions of the photopigments, determines the combination of photopigment excitations in the PCA components. Since all of the photopigment excitations are positively correlated, the first component will combine all photopigment excitations positively and account for the majority of variance (>95%), as a previous study showed [8]. The remaining components will interpret opponent relationships among the photopigment excitations. Since the remaining components account for a very small portion of variance [8], we considered the absolute value of a coefficient >0.10 as significant loading in determining the contributions of the photopigment excitations in each component. We chose this conservative cut-off criterion for significant loading in interpreting the intervariable relationships because of the low signal-to-noise ratios for the opponency components [51].

We conducted three sets of PCAs on transformed photopigment excitations: (1) a cone-opsin-based analysis that considered only the L-cone, M-cone, and S-cone opsin excitations for photopic lighting conditions; (2) a rhodopsin and cone-opsin-based analysis that included rhodopsin and S-, M- and L-cone opsin excitations for mesopic lighting conditions; and (3) a melanopsin-, rhodopsin-, and cone-opsin-based analysis that considered melanopsin, rhodopsin, and cone opsin excitations. The coefficients of the nine images were averaged for each illumination. We used a one-way ANOVA to examine the effect of the illuminants on the PCA coefficients.

A second-level PCA used postreceptoral signals by removing luminance information from untransformed photopigment excitations first; that is, $l_0 = L_0/(L_0 + M_0)$, $s_0 = S_0/(L_0 + M_0)$, $r_0 = R_0/(L_0 + M_0)$ and/or $i_0 = I_0/(L_0 + M_0)$, and then applying Eq. (1) to obtain the transformed excitations l, s, r, and i, respectively. Note $l_0 = L_0/(L_0 + M_0)$ and $s_0 = S_0/(L_0 + M_0)$ are two cardinal axes in a MacLeod & Boynton equiluminant cone chromaticity space [52], corresponding to the PC- and KC- pathways, respectively [5,53]. In such a space, luminance is specified as $L_0 M_0$ because S-cones do not contribute to $V(\lambda)$. We used the same approach to normalize rhodopsin and melanopsin excitations by cone luminance at each pixel. This second-level analysis aimed to reveal photopigment contributions to chromatic pathways. All of the analyses, including photopigment excitation calculation, PCA, and ANOVA, were carried out in MATLAB (Mathworks Inc.).

3. RESULTS

A. Cone-Opsin-Based Analysis

When L-, M-, and S-cone opsin excitations were considered, no effect of the illuminant was found over the large range of CCT illuminations. The results from the natural scenes used in the study replicated the findings from Ruderman and colleagues [8] (Table 1). That is, the

first component (labeled as "L + M + S", 97.73% of variance explained) represented cone combination in the MC-pathway, the second component [labeled as "S − (L + M)," 2.24% of variance explained] represented cone in the KC-pathway, and the third component (labeled as "M-L," 0.03% of variance explained) represented L- and M-cone opponency in the PC-pathway with minimal S-cone input. After removing luminance information, the first component (labeled as "s," 99.83% of variance explained) had input solely from s S/(L + M), which is consistent with KC-pathway mediation; the second component (labeled as "l," 0.17% of variance explained) had input only from l = L/(L + M), which is consistent with PC-pathway mediation (Table 2). These results also suggested the independence of the two chromatic axes in a cone-based chromaticity space [52].

B. Rhodopsin- and Cone-Opsin-Based Analysis

Figure 2 shows the coefficients as a function of the illuminant CCT, with each panel corresponding to a principal component [Fig. 2(a) for the first-level analysis and Fig. 2(b) for the second-level analysis]. Figure 2(a) shows that the effect of the illuminant was insignificant in the first component, but, for the other three components, the effect of the illuminant was slightly significant for some coefficients [second-principal component: $F_{(20, 168)} = 1.96$, $p = 0.011$ for S and $F_{(20, 168)} = 2.38$, p 0.002 for L; third-principal component: $F_{(20, 168)} = 2.68$, $p < 0.001$ for S and $F_{(20, 168)} = 2.36$, $p = 0.002$ for L]. Most of the variance was explained by the first component (98.2%), with coefficients for R, L, M, and S all positive and close to 0.5 (labeled as "L + M + S + R," Table 3). The combination of the photoreceptor excitations in the first component suggested a contribution to the MC-pathway. The second component had a positive S coefficient and negative M and L coefficients, while the R coefficient was negligible [labeled as "S − (L + M)," Table 3], consistent with KC-pathway mediation. The third and fourth components had L- and M-cone opponency, with R and S combined to either L or M ["(M + R) − (L + S)" and "(M + S) − (L + R)," Table 3].

The results from the second-level analysis based on l, s, and r are shown in Fig. 2(b). The illuminant effect is significant only for s [$F_{(20, 168)} = 3.8$, $p < 0.001$] and r [$F_{(20, 168)} = 3.83$, $p < 0.001$] coefficients of the first component, and for s coefficients [$F_{(20, 168)} = 3.83$, $p < 0.001$] of the second component. The first component explained most of the variance (97.86%), with positive coefficients of s and r but with a minimal l coefficient (labeled as "$s + r$," Table 4), consistent with rod contribution to the KC-pathway. For the second component, r was opposed to the combination of l and s [labeled as "$r − (l + s)$," Table 4]. For the third component, l and r were combined positively with a small s contribution (labeled as "$l + r$," Table 4).

C. Melanopsin-, Rhodopsin-, and Cone-Opsin-Based Analysis

The coefficients for the first-level analysis with S, M, L, R, and I photopigment excitations as a function of the illuminant CCT are shown in Fig. 3(a). The effect of the illuminant was significant for the second component [L: $F_{(20, 168)} = 2.59$, $p < 0.001$; S: $F_{(20, 168)} = 3.39$, $p < 0.001$] and third component [L: $F_{(20, 168)} = 2.42$, $p = 0.001$; S: $F_{(20, 168)} = 2.64$, $p < 0.001$]. As in previous analyses, most of the variance was explained by the first principal component (98.36%), in which the coefficients for all five types were similar and close to

0.5 (labeled as "L + M + S + R + I," Table 5), consistent with an MC-pathway mediation. For the second component, S and I were combined in opposition to M and L with an insignificant R contribution [labeled as "(S + I) − (L + M)," Table 5], suggesting a melanopsin contribution to the KC-pathway. The third to fifth components all had L and M opponency, but S, R, and I were combined to L or M differently (Table 5).

For the second-level analysis [Fig. 3(b)], the effect of the illuminants was significant for some coefficients of the first component [i: $F_{(20, 168)}$ 3.47, $p < 0.001$, s: $F_{(20, 168)} = 4.09$, $p < 0.001$; r: $F_{(20, 168)} = 4.33$, $p < 0.001$], the second component [s: $F_{(20, 168)} = 5.18$, $p < 0.001$; r: $F_{(20, 168)} = 2.65$, $p < 0.001$], and the third component [i: $F_{(20, 168)} = 1.73$, $p = 0.03$]. The first principal component explained most of the variance (97.05%) and consisted of positive coefficients for s, r, and i with an insignificant l contribution (labeled as "$s + r + i$," Table 6). The second component had positive coefficients for i and r and negative coefficients for s and l [labeled as "$(r + i − (l + s)$," Table 6]. The third component had and similar coefficients for i and l, and negative coefficients for r and s [labeled as "$(l + i) − (s + r)$" Table 6]. The fourth component had positive coefficients for l and r and negative coefficients for i with an insignificant contribution of s (labeled as "$l + r − i$," Table 6).

4. DISCUSSION

Using PCAs, we were able to obtain efficient combinations of the excitations of five known photopigments in primates (L-, M-, and S-cone opsins, rhodopsin, and melanopsin), constrained by natural image statistics. The current analysis only focused on photopigment spectral responses, without considering large differences in retinal distributions [54], and spatial, temporal, and contrast response characteristics among the photopigments (for review, see [55]). Nevertheless, our findings can be used to infer how the environmental constraints limit the formation of postreceptoral pathways based on photopigment spectral responses, as it has been shown that adding spatial information into cone responses does not change cone combination patterns in PCA [8]. Our results can also be useful in the development and testing of new hypotheses on the contributions of rhodopsin, cone opsins, and melanopsin to visual functions through psychophysical, anatomical, or physiological experiments [6].

A. Interpretation of the Results

Analysis based on only L-, M-, and S-cone opsin excitations revealed three principal components that are consistent with cone combinations in the MC-, KC-, and PC-pathways [8]. Further, when analyses were repeated using $l = L/(L + M)$ and $s = S/(L + M)$ to remove luminance information, the components obtained were consistent with two independent cardinal axes in a cone-based chromaticity diagram [52]; that is, $L/(L + M)$ and $S/(L + M)$.

When rhodopsin excitation was considered in the analysis, the first two components revealed by the cone-opsin-based analysis were maintained with a strong rod contribution to the MC-pathway ("L + M + S + R") and a weak contribution to the KC-pathway after removing luminance information (i.e., $\sim 0.95s + 0.3r$, Table 4). The joint contributions of rods and cones in the MC-pathway is consistent with previous psychophysical measurements [26,56] and physiological studies [19,22]. The rod contribution to the KC-

pathway was also supported by psychophysical [26,27] and recent physiological studies [24,25]. Interestingly, our analysis revealed two components that opposed L- and M-cones, with rods and S-cone combined differently with L- or M-cones ["(M + R) − (L + S)" or "(M + S) − (L + R)," Table 3]. We referred to these two components as "PC-like" components because they largely indicate the opponency between L- and M-cone inputs. In these two components, rods are combined with either M-cones ["(M + R) − (L + S)"] or L-cones ["(M + S) − (L + R)"]. Given that rods contact cones through gap junctions at mesopic light levels [54,57], it is not surprising that rods and L- and M-cones were combined in the same sign. A psychophysical study has suggested that rods contribute to color perception as an analog of M cones [27], which is consistent with the "(M + R) − (L + S)" component. However, these two components [as well as the "$r − (l + s)$" component in the analysis with luminance removed, Table 4] also suggest that S-cones are combined with L- or M-cones, and this cannot be explained in terms of independence of the two cardinal axes. Primate retinal ganglion cell recording suggests lack of S-cone input to PC-pathway neurons [3]. However, S-OFF neurons in the macaque LGN show L-cone signals oppose the combination of S- and M-cone signals [58]. In the primary visual cortex of primates, there are cells that prefer noncardinal color axes [59], as suggested by psychophysical [60] and fMRI studies [61]. Also, recent S-cone discrimination measurements showed a channel-preferred combination of L and S cone excitation [62,63]. It is possible that adding rod signals in the analysis provides additional constraints to L-, M-, and S-cone excitations, leading to new combinations of cone inputs, probably at an early cortical processing stage [61].

Results from the analyses with inclusion of melanopsin together with rhodopsin and cone opsins are qualitatively similar to those obtained with rhodopsin- and cone-opsin-based analyses (Tables 3 and 4). That is, the analyses revealed a component signaling the sum of all the photoresponses ("L + M + S + R + I") in the MC-pathway, and the opponency of S cones and the sum of L- and M-cones in the KC-pathway, with rhodopsin and melanopsin contributing as the same sign as S-cone opsin (Tables 5 and 6). Rhodopsin and melanopsin also contribute to components that oppose L- and M-cone opsins, with rhodopsin, melanopsin, and S-cone opsin combined differently with L- or M-cone opsins. One important role of ipRGCs is to provide retinal inputs for controlling pupil responses and circadian rhythms [34]. Therefore, the best-known melanopsin function, together with rhodopsin and cone-opsins, is to respond to irradiance levels, as suggested by the first principal component of our analysis. The ipRGCs are anatomically and physiologically distinctive from the parasol, midget, and small bistratified ganglion cells in the three major retinogeniculate pathways [33]. ipRGCs project to the SCN and OPN primarily to control the biological clock and pupil responses. However, ipRGCs also project to LGN. If there is any input from melanopsin signals to the MC-, PC-, or KC-pathways, it is likely that the signals are combined at the LGN level or even a later stage. It has been reported that melanopsin contributes to brightness perception [38] or alters visual sensitivity [39]. However, probably due to the differences in spatial, temporal, chromatic, and contrast response characteristics between melanopsin and rhodopsin or cone opsins, the contribution of melanopoin to visual perception is probably very weak.

B. Illuminant Effect

A large range of illuminants was tested; however, no effect of the illuminants in most of the coefficients was found. It has been reported that an image with a flat radiance spectrum produced qualitatively similar results to the set of natural images [8]. Therefore, the invariance with illuminants can be explained by the spectral position of the photoreceptor distributions, which is the main foundation for signal redundancy removal [8,9,64]. When rhodopsin and melanopsin are incorporated in the analysis, small effects of illuminations on component weighting are observed, particularly those with low CCT for mesopic light illuminations (such as a moon light or dawn light). These results are consistent with the report that the strength of the rod-cone coupling could be affected during the phase of the day [65], further suggesting the importance of rods under dim illumination conditions in visual processing.

C. Implications of Explained Component Variance

In our analysis, the first few principal components accounted for most of the variance in the natural scene data. The first component from all the analyses (Tables 1,3,5) was related to luminance and explained over 97% of the variance in the data. From an ecological perspective, this makes sense since most of the information in the visual environment corresponds to changes in reflectance. This characteristic is exploited by most of the species deprived of trichromatic vision. The second component that accounted for the second highest amount of the variance was related to the KC-pathway, even considering rhodopsin and melanopsin. This indicated that the most important chromatic variation in the natural environment is in the "blue-yellow" axis, which is consistent with the hypothesis that the first chromatic pathway that appeared in early mammals originated in the small bistratified ganglion cells in the KC-pathway [66]. The component that can be assigned to the PC- or (PC-like) pathway for LM cone opponency explained a very small amount of the variance in the data, suggesting that the variation of the data in the "red-green" axis was relatively small in natural images. It has been suggested that signals from the "red-green" channel in primates are essential for the discrimination of nutritional leaves [67], but not for identification fruits, which can also be discriminated by the luminance and "blue-yellow" channels [67,68]. This is probably why only some primates have more recently evolved different L- and M-cone mosaics. Indeed, an additional analysis considering only M-cone and S-cone opsins, rhodopsin, and melanopsin (data not shown) has preserved the photopigment combination patterns attributed to MC- and KC-pathways.

Acknowledgments

REFERENCES

1. Lee BB. "Visual pathways and psychophysical channels in the primate,". J. Physiol. 2011; 589:41–47. [PubMed: 20724364]

2. Dacey DM. "Parallel pathways for spectral coding in primate retina,". Annu. Rev. Neurosci. 2000; 23:743–775. [PubMed: 10845080]

3. Sun H, Smithson HE, Zaidi Q, Lee BB. "Specificity of cone inputs to macaque retinal ganglion cells,". J. Neurophysiol. 2006; 95:837–849. [PubMed: 16424455]

4. Derrington AM, Lennie P. "Spatial and temporal contrast sensitivities of neurones in lateral geniculate nucleus of macaque,". J. Physiol. 1984; 357:219–240. [PubMed: 6512690]

5. Lee BB, Pokorny J, Smith VC, Martin PR, Valberg A. "Luminance and chromatic modulation sensitivity of macaque ganglion cells and human observers,". J. Opt. Soc. Am. A. 1990; 7:2223–2236. [PubMed: 2090801]

6. Geisler WS. "Visual perception and the statistical properties of natural scenes,". Annu. Rev. Psychol. 2008; 59:167–192. [PubMed: 17705683]

7. Simoncelli EP, Olshausen BA. "Natural image statistics and neural representation,". Annu. Rev. Neurosci. 2001; 24:1193–1216. [PubMed: 11520932]

8. Ruderman DL, Cronin TW, Chiao C-C. "Statistics of cone responses to natural images: implications for visual coding,". J. Opt. Soc. Am. A. 1998; 15:2036–2045.

9. Buchsbaum G, Gottschalk A. "Trichromacy, opponent colours coding and optimum colour information transmission in the retina,". Proc. R. Soc. B. 1983; 220:89–113. [PubMed: 6140684]

10. Jocobs GH. "Recent progress in understanding mammalian color vision,". Ophthalmic Physiolog. Opt. 2010; 30:422–434.

11. Jacobs GH, Deegan JF II, Neitz J, Crognale MA, Neitz M. "Photopigments and color vision in the nocturnal monkey, Aotus,". Vis. Res. 1993; 33:1773–1783. [PubMed: 8266633]

12. Osorio D, Vorobyev M. "A review of the evolution of animal colour vision and visual communication signals,". Vis. Res. 2008; 48:2042–2051. [PubMed: 18627773]

13. Masland RH. "The fundamental plan of the retina,". Nat. Neurosci. 2001; 4:877–886. [PubMed: 11528418]

14. Daw NW, Jensen EJ, Brunken WJ. "Rod pathways in the mammalian retinae,". Trends Neurosci. 1990; 13:110–115. [PubMed: 1691871]

15. Sharpe LT, Stockman A. "Rod pathways: the importance of seeing nothing,". Trends Neurosci. 1999; 22:497–504. [PubMed: 10529817]

16. Buck, SL. "The interaction of rod and cone signals: pathways and psychophysics," in. In: Werner, JS.; Chalupa, LM., editors. The New Visual Neurosciences. MIT; 2014. p. 485-497.

17. Gouras P, Link K. "Rod and cone interaction in dark-adapted monkey ganglion cells,". J. Physiol. 1966; 184:499–510. [PubMed: 4958644]

18. Virsu V, Lee BB. "Light adaptation in cells of macaque lateral geniculate nucleus and its relation to human light adaptation,". J. Neurophysiol. 1983; 50:864–878. [PubMed: 6631467]

19. Lee BB, Smith VC, Pokorny J, Kremers J. "Rod inputs to macaque ganglion cells,". Vis. Res. 1997; 37:2813–2828. [PubMed: 9415362]

20. Virsu V, Lee BB, Creutzfeldt OD. "Mesopic spectral responses and the Purkinje shift of macaque lateral geniculate cells,". Vis. Res. 1987; 27:191–200. [PubMed: 3576979]

21. Purpura K, Kaplan E, Shapley RM. "Background light and the contrast gain of primate P and M retinal ganglion cells,". Proc. Natl. Acad. Sci. USA. 1988; 85:4534–4537. [PubMed: 3380804]

22. Cao D, Lee BB, Sun H. "Combination of rod and cone inputs to in the parasol ganglion cells of the magnocellular pathway,". J. Vis. 2010; 10(2):11. [PubMed: 20462312]

23. Wiesel T, Hubel DH. "Spatial and chromatic interactions in the lateral geniculate body of the rhesus monkey,". J. Neurophysiol. 1966; 29:1115–1156. [PubMed: 4961644]

24. Crook JD, Davenport CM, Peterson BB, Packer O, Detwiler PB, Dacey DM. "Parallel ON and OFF cone bipolar inputs establish spatially coextensive receptive field structure of blue-yellow ganglion cells in primate retina,". J. Neurosci. 2009; 29:8372–8387. [PubMed: 19571128]

25. Field GD, Greschner M, Gauthier JL, Rangel C, Shlens J, Sher A, Marshak DW, Litke AM, Chichilnisky EJ. "High-sensitivity rod photoreceptor input to the blue-yellow color opponent pathway in macaque retina,". Nat. Neurosci. 2009; 12:1159–1164. [PubMed: 19668201]

26. Cao D, Pokorny J, Smith VC, Zele AJ. "Rod contributions to color perception: linear with rod contrast,". Vis. Res. 2008; 48:2586–2592. [PubMed: 18561973]

27. Cao D, Pokorny J, Smith VC. "Matching rod percepts with cone stimuli,". Vis. Res. 2005; 45:2119–2128. [PubMed: 15845243]

28. Buck SL, Knight RF, Bechtold J. "Opponent-color models and the influence of rod signals on the loci of unique hues,". Vis. Res. 2000; 40:3333–3344. [PubMed: 11058732]

29. Barlow HB. "What causes trichromacy? A theoretical analysis using comb-filtered spectra,". Vis. Res. 1982; 22:635–643. [PubMed: 6981244]

30. Van Hateren J. "Spatial, temporal and spectral pre-processing for colour vision,". Proc. R. Soc. Lond. 1993; 251:61–68.

31. Berson DM, Dunn FA, Takao M. "Phototransduction by retinal ganglion cells that set the circadian clock,". Science. 2002; 295:1070–1073. [PubMed: 11834835]

32. Hattar S, Liao HW, Takao M, Berson DM, Yau KW. "Melanopsin-containing retinal ganglion cells: architecture, projections, and intrinsic photosensitivity,". Science. 2002; 295:1065–1070. [PubMed: 11834834]

33. Dacey DM, Liao H, Peterson B, Robinson F, Smith VC, Pokorny J, Yau KW, Gamlin PD. "Melanopsin-expressing ganglion cells in primate retina signal color and irradiance and project to the LGN,". Nature. 2005; 433:749–754. [PubMed: 15716953]

34. McDougal D, Gamlin P. "Pupillary control pathways,". The Senses: A Comprehensive Reference. 2008; 1:521–536.

35. Lall GS, Revell VL, Momiji H, Al Enezi J, Altimus CM, Güler AD, Aguilar C, Cameron MA, Allender S, Hankins MW. "Distinct contributions of rod, cone, and melanopsin photoreceptors to encoding irradiance,". Neuron. 2010; 66:417–428. [PubMed: 20471354]

36. Hattar S, Lucas RJ, Mrosovsky N, Thompson S, Douglas R, Hankins MW, Lem J, Biel M, Hofmann F, Foster RG. "Melanopsin and rod–cone photoreceptive systems account for all major accessory visual functions in mice,". Nature. 2003; 424:75–81.

37. Ruby NF, Brennan TJ, Xie X, Cao V, Franken P, Heller HC, O'Hara BF. "Role of melanopsin in circadian responses to light,". Science. 2002; 298:2211–2213. [PubMed: 12481140]

38. Brown TM, Tsujimura S.-i. Allen AE, Wynne J, Bedford R, Vickery G, Vugler A, Lucas RJ. "Melanopsin-based brightness discrimination in mice and humans,". Curr. Biol. 2012; 22:1134–1141. [PubMed: 22633808]

39. Horiguchi H, Winawer J, Dougherty RF, Wandell BA. "Human trichromacy revisited,". Proc. Natl. Acad. Sci. USA. 2013; 110:E260–E269. [PubMed: 23256158]

40. Foster DH, Amano K, Nascimento S, Foster MJ. "Frequency of metamerism in natural scenes,". J. Opt. Soc. Am. A. 2006; 23:2359–2372.

41. Nascimento S, Ferreira FP, Foster DH. "Statistics of spatial cone-excitation ratios in natural scenes,". J. Opt. Soc. Am. A. 2002; 19:1484–1490.

42. Nascimento S, Masuda O. "Psychophysical optimization of lighting spectra for naturalness, preference, and chromatic diversity,". J. Opt. Soc. Am. A. 2012; 29:A144–A151.

43. Linhares JMM, Nascimento SMC. "A chromatic diversity index based on complex scenes,". J. Opt. Soc. Am. A. 2012; 29:A174–A181.

44. Wyszecki, G.; Stiles, WS. Color Science—Concepts and Methods, Quantitative Data and Formulae. 2nd ed. Wiley; 1982. p. 1-950.

45. Stair R, Johnston R. "Ultraviolet spectral radiant energy reflected from the moon,". J. Res. Nat. Bureau Stan. 1953; 51:81–84.

46. Hernandez-Andres J, Lee RL, Romero J. "Calculating correlated color temperatures across the entire gamut of daylight and skylight chromaticities,". Appl. Opt. 1999; 38:5703–5709. [PubMed: 18324081]

47. Smith VC, Pokorny J. "Spectral sensitivity of the foveal cone photopigments between 400 and 500 nm,". Vis. Res. 1975; 15:161–171. [PubMed: 1129973]

48. Shapiro AG, Pokorny J, Smith VC. "Cone-rod receptor spaces, with illustrations that use CRT phosphor and light-emitting-diode spectra,". J. Opt. Soc. Am. A. 1996; 13:2319–2328.

49. al Enezi J, Revell V, Brown T, Wynne J, Schlangen L, Lucas R. "A "melanopic" spectral efficiency function predicts the sensitivity of melanopsin photoreceptors to polychromatic lights,". J. Biol. Rhythms. 2011; 26:314–323. [PubMed: 21775290]

50. Jolliffe, I. "Principal component analysis,". In: Everitt, BS.; Howell, D., editors. Encyclopedia of Statistics in Behavioral Science. Wiley Online Library; 2005.

51. Richman MB. "A cautionary note concerning a commonly applied eigenanalysis procedure,". Tellus B. 1988; 40:50–58.

52. MacLeod DIA, Boynton RM. "Chromaticity diagram showing cone excitation by stimuli of equal luminance,". J. Opt. Soc. Am. 1979; 69:1183–1185. [PubMed: 490231]

53. Derrington AM, Krauskopf J, Lennie P. "Chromatic mechanisms in lateral geniculate nucleus of macaque,". J. Physiol. 1984; 357:241–265. [PubMed: 6512691]

54. Li PH, Verweij J, Long JH, Schnapf JL. "Gap-junctional coupling of mammalian rod photoreceptors and its effect on visual detection,". J. Neurosci. 2012; 32:3552–3562. [PubMed: 22399777]

55. Hatori M, Panda S. "The emerging roles of melanopsin in behavioral adaptation to light,". Trends Mol. Med. 2010; 16:435–446. [PubMed: 20810319]

56. Sun H, Pokorny J, Smith VC. "Rod-cone interactions assessed in inferred postreceptoral pathways,". J. Vis. 2001; 1(1):42–54. [PubMed: 12678613]

57. Hornstein EP, Verweij J, Li PH, Schnapf JL. "Ga-pjunctional coupling and absolute sensitivity of photoreceptors in Macaque retina,". J. Neurosci. 2005; 25:11201–11209. [PubMed: 16319320]

58. Tailby C, Solomon SG, Lennie P. "Functional asymmetries in visual pathways carrying S-cone signals in macaque,". J. Neurosci. 2008; 28:4078–4087. [PubMed: 18400907]

59. Conway BR. "Spatial structure of cone inputs to color cells in alert macaque primary visual cortex (v-1),". J. Neurosci. 2001; 21:2768–2783. [PubMed: 11306629]

60. Webster MA, Mollon JD. "Changes in colour appearance following post-receptoral adaptation,". Nature. 1991; 349:235–238. [PubMed: 1987475]

61. Goddard E, Mannion DJ, McDonald JS, Solomon SG, Clifford CW. "Combination of subcortical color channels in human visual cortex,". J. Vis. 2010; 10(5):25. [PubMed: 20616126]

62. Danilova MV, Mollon J. "Parafoveal color discrimination: a chromaticity locus of enhanced discrimination,". J. Vis. 2010; 10(1):4. [PubMed: 20143897]

63. Cao D. "S-cone discrimination in the presence of two adapting fields: data and model,". J. Opt. Soc. Am. A. 2014; 31:A65–A74.

64. Shevell SK, Kingdom FA. "Color in complex scenes,". Annu. Rev. Psychol. 2008; 59:143–166. [PubMed: 18154500]

65. Ribelayga C, Cao Y, Mangel SC. "The circadian clock in the retina controls rod-cone coupling,". Neuron. 2008; 59:790–801. [PubMed: 18786362]

66. Regan BC, Julliot C, Simmen B, Viénot F, Charles-Dominique P, Mollon JD. "Fruits, foliage and the evolution of primate colour vision,". Philos. Trans. R. Soc. B. 2001; 356:229–283.

67. Dominy NJ, Lucas PW. "Ecological importance of trichromatic vision to primates,". Nature. 2001; 410:363–366. [PubMed: 11268211]

68. Sumner P, Mollon J. "Chromaticity as a signal of ripeness in fruits taken by primates,". J. Exp. Biol. 2000; 203:1987–2000. [PubMed: 10851116]
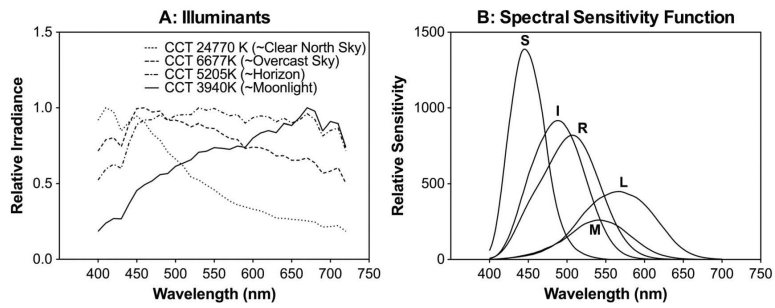
Fig. 1.

Illuminants and photopigment spectral sensitivity functions. (a) Spectral distributions correspond to four representative "D" illuminants for natural skylights. (b) Normalized spectral sensitivity functions of rhodopsin (R), L-, M-, S-cone opsins, and melanopsin (I).
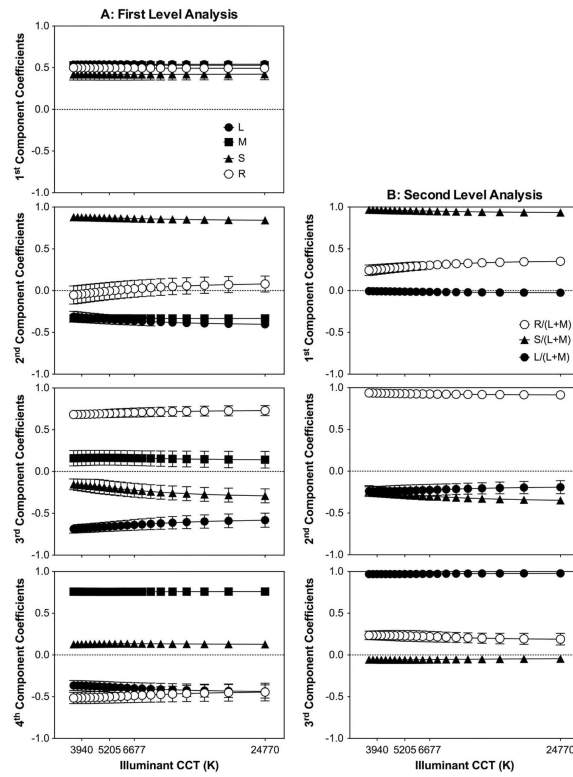
Fig. 2.

Rhodopsin- and cone-opsin-based analysis. The coefficients values averaged for the nine images versus the CCT of the "D" illuminants are shown. Each panel corresponds to one of the four principal components corresponding to the first level of analysis (A, left column), or to one of the three principal components corresponding to the second level of analysis (B, right column). Error bars are the standard deviation of the results for the nine images.
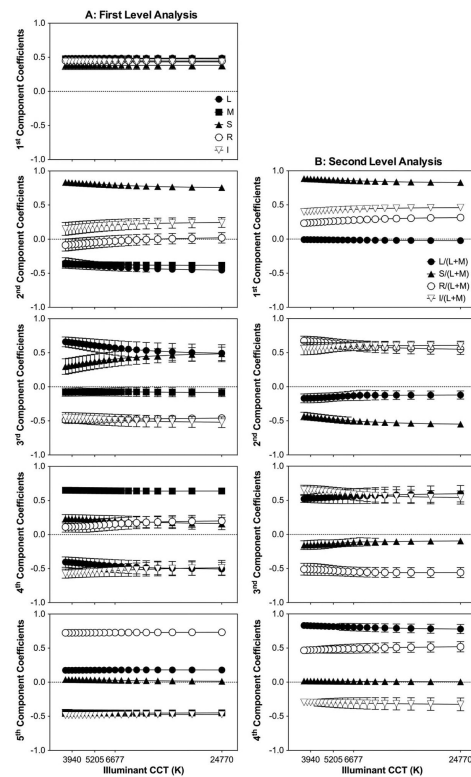
Fig. 3.
Melanopsin-, rhodopsin-, and cone-opsin-based analysis. The coefficients values averaged for the nine images versus the CCT of the "D" illuminants are shown. Each panel corresponds to one of the five principal components corresponding to the first level of analysis (A, left column), or to one of the four principal components corresponding to the second level of analysis (B, right column). Error bars are the standard deviation of the results for the nine images.

Table 1

Averaged Coefficients Values Across the Illuminant from the First Level of Analysis for the Cone-Opsin-Based Analysis[a]

Component	L	M	S	Variance Explained (%)	Notation[b]	Pathway
1st	0.62	0.61	0.48	97.73	L + M + S	MC
2nd	−0.35	−0.33	0.87	2.24	S − (L + M)	KC
3rd	−0.7	0.72	−0.03	0.03	M − L	PC

[a]No effect of the illuminant was found over the large range of CCT illuminations.

[b]Notation indicates combinations of variables with coefficients >0.10.

Table 2

Averaged Coefficient Values Across the Illuminant from the Second Level of Analysis for the Cone-Opsin-Based Analysis[a]

Component	*l*	*s*	Variance Explained (%)	Notation[b]	Pathway
1st	−0.02	0.99	99.83	*s*	KC
2nd	0.99	0.02	0.17	*l*	PC

[a] No effect of the illuminant was found over the large range of CCT illuminations.

[b] Notation indicates combinations of variables with coefficients >0.10.

Table 3

Averaged Coefficient Values Across the Illuminant from the First Level of Analysis for the Rhodopsin- and Cone-Opsin-Based Analysis

Component	L	M	S	R	Variance Explained (%)	Notation[a]	Pathway
1st	0.54	0.53	0.42	0.5	98.19	L + M + S + R	MC
2nd	−0.36	−0.33	0.86	0.01	1.74	S − (L + M)	KC
3rd	−0.64	0.16	−0.21	0.7	0.06	(M + R) − (L + S)	PC-like
4th	−0.4	0.76	0.13	−0.47	0.01	(M + S) − (L + R)	PC-like

[a]Notation indicates combinations of variables with coefficients >0.10.

Table 4

Averaged Coefficients Values Across the Illuminant from the Second Level of Analysis for the Rhodopsin- and Cone-Opsin-Based Analysis

Component	l	s	r	Variance Explained (%)	Notation[a]	Pathway
1st	−0.01	0.95	0.3	97.86	$s + r$	KC
2nd	−0.23	−0.29	0.93	2.10	$r − (l + s)$	PC-like
3rd	0.95	−0.1	0.2	0.04	$l + r$	PC-like

[a]Notation indicates combinations of variables with coefficients >0.10.

Table 5

Averaged Coefficients Values Across the Illuminant from the First Level of Analysis for the Melanopsin-, Rhodopsin-, and Cone-Opsin-Based Analysis

Component	L	M	S	R	I	Variance Explained (%)	Notation[a]	Pathway
1st	0.49	0.48	0.38	0.45	0.43	98.36	L + M + S + R + I	MC
2nd	−0.4	−0.38	0.8	−0.04	0.2	1.56	(S + I) − (L + M)	KC
3rd	0.59	−0.08	0.39	−0.48	−0.48	0.07	(L + S) − (R + I)	Unknown
4th	−0.45	0.64	0.21	0.15	−0.54	0.01	(M + S + R) − (L + I)	PC-like
5th	0.18	−0.45	0.03	0.73	−0.48	<0.01	(L + R) − (M + I)	PC-like

[a]Notation indicates combinations of variables with coefficients >0.10.

Table 6

Averaged Coefficients Values Across the Illuminant from the Second level of Analysis for the Melanopsin-, Rhodopsin-, and Cone-Opsin-Based Analysis

Component	l	s	r	i	Variance Explained (%)	Notation[a]	Pathway
1st	−0.01	0.86	0.27	0.43	97.05	$s + r + i$	KC
2nd	−0.14	−0.49	0.62	0.58	2.80	$(r + i) − (l + s)$	Unknown
3rd	0.56	−0.13	−0.54	0.6	0.14	$(l + i) − (s + r)$	PC-like
4th	0.81	0.01	0.49	−0.31	0.01	$l + r − i$	PC-like

[a]Notation indicates combinations of variables with coefficients >0.10.